CHALMERS
UNIVERSITY OF TECHNOLOGY

Multiple Model Poisson Multi-Bernoulli Mixture for 5G Mapping

Multiple Model Poisson Multi-Bernoulli Mixture for 5G Mapping

Hyowon Kim[1], Henk Wymeersch[2], Sunwoo Kim[1]
[1]Department of Electronics and Computer Engineering, Hanyang University, South Korea
[2]Department of Electronic Engineering, Chalmers University of Technology, Sweden
[1]{khw870511, remero}@hanyang.ac.kr, [2]henkw@chalmers.se

Abstract

In this paper, we evaluate and compare the multiple model Poisson multi-Bernoulli mixture (MM-PMBM) and the multiple model probability hypothesis density (MM-PHD) filters for mapping a propagation environment, specified by multiple types objects, using 5G millimeter-wave signals. To develop the MM-PMBM applicable to 5G scenarios, we design the density representation, data structure, and implementation strategy. From the simulation results, it is demonstrated that the MM-PMBM captures the objects and is robust to both missed detections and false alarm compared to the MM-PHD.

I. Introduction

5G mapping has several specific challenges, due to imperfect detection process at the mobile receiver, limited and time-varying detection range with the variable field-of-view (FoV), false detections (due to clutter and channel estimation errors), different object types, and uncertainty of data association. To handle these challenges, random-finite-set (RFS) based methods provide a powerful framework and include the probability hypothesis density (PHD) [1] and Poisson multi Bernoulli mixture (PMBM) filters [2]. The authors in [3] developed a multiple model PHD (MM-PHD) filter, which can map the environment, but suffers from performance degradation when the objects are closer.

In this paper, we introduce the multiple model PMBM (MM-PMBM) and its implementation to deal with closely located objects. We demonstrate that the MM-PMBM has a mapping gain over MM-PHD and is more robust to both missed detections and false alarm.

II. Models

We consider a moving user equipment (UE) with known state. The UE state at time k is denoted by $\mathbf{s}_k$ and includes the 3D position, heading, and turn rate [4]. We adopt the propagation environment model from [4], characterized by the base station (BS), virtual anchors (VAs) that model large reflecting surfaces, and scattering points (SPs) that model small objects. We denote object location by $\mathbf{x} = [x, y, z]^\mathsf{T}$ with the spatial density $f(\mathbf{x})$, and object type by $m \in \{\text{BS}, \text{VA}, \text{SP}\}$, and an RFS of the objects with tuples $(\mathbf{x}, m)$ by $\mathcal{X}$ with the set density $f(\mathcal{X})$. At time k, the vehicle receives multipath signals, and signal detections follow a detection probability, modeled as $p_{\text{D},k}(\mathbf{s}_k, \mathbf{x}, m) \in [0,1]$ with the FoV as depicted in Fig. 1. By the channel estimation routine at the receiver, the vehicle observes measurements, denoted by an RFS $\mathcal{Z}_k = \{z_k^1, \dots, z_k^{J_k}\}$, where J_k is the number of detected signal paths. We model each measurement element as $z_k^j = h(\mathbf{s}_k, \mathbf{x}_i, m_i) + \mathbf{r}_k^j$, where $h(\mathbf{s}_k, \mathbf{x}_i, m_i) = [\tau_k^j, (\boldsymbol{\theta}_k^j)^\mathsf{T}, (\boldsymbol{\phi}_k^j)^\mathsf{T}]^\mathsf{T}$, and $\mathbf{r}_k^j \sim \mathcal{N}(\mathbf{0}, \mathbf{R})$ denotes the measurement noise. Here, τ_k^j, $\boldsymbol{\theta}_k^j$, $\boldsymbol{\phi}_k^j$, and $\mathbf{R}$ respectively denote a time-of-arrival (TOA), direction-of-arrival (DOA) in azimuth and elevation, direction-of-departure (DOD) in azimuth and elevation, and known covariance matrix. We also consider clutter, generated by either false alarm (e.g., channel estimation error) or transient object (e.g., passing car or people) as measurement elements. Note that the association between the measurement $\mathbf{z}_{k,l}$ and the object identifier i, location $\mathbf{x}_i$ and type m_i are unknown.

III. MM-PMBM for 5G Mapping

Density Representation: We introduce the PMBM density [3].

$$f_{\text{PMBM}}(\mathcal{X}) = \sum_{\mathcal{X}^\text{U} \uplus \mathcal{X}^\text{D} = \mathcal{X}} f_{\text{Poi}}(\mathcal{X}^\text{U}) f_{\text{PMBM}}(\mathcal{X}^\text{D}), \tag{1}$$

where $f_{\text{Poi}}(\mathcal{X}^\text{U})$ denotes a Poisson density for the objects which have never been detected, $f_{\text{PMBM}}(\mathcal{X}^\text{D})$ denotes an MBM density for the previously and newly detected objects, and $\uplus$ denotes the disjoint union. Here, $\mathcal{X}^\text{U}$ denotes a set of undetected objects, and $\mathcal{X}^\text{D}$ denotes a set of previously or newly detected objects. The Poisson density is defined as

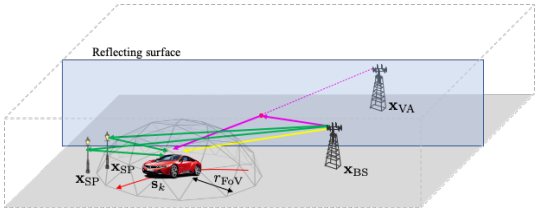

Fig. 1. Propagation environment, characterized by the BS, VA, and two SPs.

$$f_{\text{Poi}}(\mathcal{X}) = e^{-\mu} \prod_{\mathbf{x} \in \mathcal{X}} \mu f(\mathbf{x}), \tag{2}$$

where μ is the mean of the Poisson distribution for the set cardinality, and intensity function is defined as $\lambda(\mathbf{x}) = \mu f(\mathbf{x})$. The MBM density is defined as

$$f_{\text{MBM}}(\mathcal{X}) = \sum_{\text{h}} w^h f_{\text{MB}}^h(\mathcal{X}), \tag{3}$$

where h denotes an index of global hypotheses, w^h is the weight of $f_{\text{MB}}^h(\mathcal{X})$, and $\sum_h w^h = 1$. Here, the MB density $f_{\text{MB}}(\mathcal{X})$ is represented as

$$f_{\text{MB}}(\mathcal{X}) = \sum_{\mathcal{X}^1 \uplus \dots \uplus \mathcal{X}^n = \mathcal{X}} \prod_{i=1} f_{\text{B}}(\mathcal{X}^i). \tag{4}$$

The Bernoulli density $f_{\text{B}}(\mathcal{X})$ is defined for $|\mathcal{X}|$ as

$$f_{\text{B}}(\mathcal{X}) = \begin{cases} 1 - r, & \mathcal{X} = \emptyset, \\ r f(\mathbf{x}), & \mathcal{X} = \{\mathbf{x}\}, \end{cases} \tag{5}$$

Data Structure: We explicitly need to consider data association, and thus we update both global hypotheses and hypotheses tree. The previous global hypotheses is represented by $\mathbf{H}_{k-1} \in \mathbb{R}^{H_{k-1} \times I_{k-1}}$, where H_{k-1} indicates the number of previous global hypotheses, and I_{k-1} indicates the number of detected potential objects at previous time, with $H_{k-1}(h, j)$ (row h, column i of H_{k-1}) denoting the data association of the h-th global hypothesis and the j-th track at time $k-1$. The weight of global hypotheses is represented by $\mathbf{w}_{k-1} = [w_{k-1}^1, \dots, w_{k-1}^{H_{k-1}}]^\mathsf{T}$, and its h-th element w_{k-1}^h is the weight of h-th global hypothesis. We adopt the track-oriented implementation [3]. Then, there are I_{k-1} single tracks, and track i consists of H_{k-1} local hypotheses. Data structure at the end of time $k-1$ consists of undetected object density, and detected object, and global hypotheses: $\lambda_{\text{u},k-1}(\mathbf{x}, m)$;

$$\left\{ \left\{ \left\{ f_{\text{u},k-1}^{i,h^i}(\mathbf{x}, m) \right\}_{m=\{\text{VA},\text{SP}\}}, r_{\text{u},k-1}^{i,h^i} \right\}_{h^i=1}^{H_{k-1}^i} \right\}_{i=1}^{I_{k-1}}, \{w_{k-1}^h\}_{h=1}^{H_{k-1}}; \mathbf{H}_{k-1}$$

(global hypotheses matrix).

Prediction: For the undetected objects, the intensity is predicted as $\lambda_{\text{p},k-1}(\mathbf{x}, m) = p_\text{S}(m)\lambda_{\text{u},k-1}(\mathbf{x}, m) + \lambda_\text{B}(\mathbf{x}, m)$, where p_S is the survival probability, and $\lambda_\text{B}(\mathbf{x}, m)$ is a birth intensity, which is also represented as a scaled uniform distribution [5]. For the detected objects, the Bernoulli components for local hypothesis h of track i is predicted as

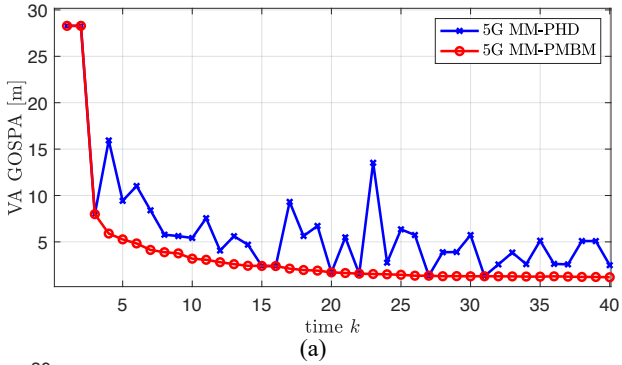

(a)

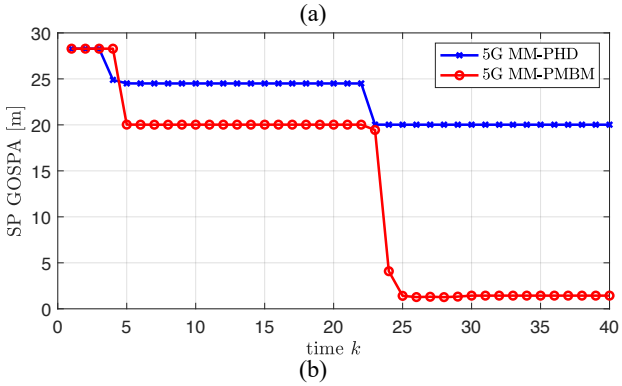

(b)

Fig. 2. Average GOSPA of the (a) VA and (B) SP for the 5G MM-PMBM compared to the 5G MM-PHD.

$$f_{\mathrm{p},k-1}^{i,h^i}(\mathbf{x},m)=\frac{p_{\mathrm{S}}(m)f_{\mathrm{u},k-1}^{i,h^i}(\mathbf{x},m)}{\sum_{m'}\int p_{\mathrm{S}}(m')f_{\mathrm{u},k-1}^{i,h^i}(\mathbf{x}',m')\mathrm{d}\mathbf{x}'} \tag{6}$$

$$r_{\mathrm{p},k-1}^{i,h^i}=r_{\mathrm{u},k-1}^{i,h^i}\sum_{m}\int p_{\mathrm{S}}(m)f_{\mathrm{u},k-1}^{i,h^i}(\mathbf{x},m)\mathrm{d}\mathbf{x}. \tag{7}$$

Correction: The correction step consists of the four parts as follows: part i) misdetections of the undetected objects; part ii) detections of the undetected objects, which are potentially detected for the first time or clutter; part iii) misdetections of the previously detected objects; and part iv) detections of the previously detected objects. In part i), the intensity function is computed as $\lambda_{\mathrm{u},k-1}(\mathbf{x},m)=(1-p_{\mathrm{D},k}(\mathbf{x},m))\lambda_{\mathrm{p},k-1}(\mathbf{x},m)$, where $p_{\mathrm{D},k}(\mathbf{x},m)$ is an adaptive detection probability. In part ii), each MBM component for the measurement $\mathbf{z}_k^j\in\mathcal{Z}_k$ are calculated as

$$f_{\mathrm{u},k}^{j}(\mathbf{x},m)=\frac{p_{\mathrm{D},k}(\mathbf{x},m)\lambda_{\mathrm{p},k}(\mathbf{x},m)g(\mathbf{z}_k^j|\mathbf{x},m)}{\sum_{m'}e_k^j(m')}, \tag{8}$$

$$r_{\mathrm{u},k}^{j}=\frac{\sum_m e_k^j(m)}{v_k^j(\{\mathbf{z}_k^j\})},\ w_k^j=v_k^j(\{\mathbf{z}_k^j\}), \tag{9}$$

where $e_k^j(m)=\int p_{\mathrm{D},k}(\mathbf{x},m)\lambda_{\mathrm{p},k}(\mathbf{x},m)g(\mathbf{z}_k^j|\mathbf{x},m)\mathrm{d}\mathbf{x}$, and $v_k^j(\{\mathbf{z}_k^j\})=\sum_m e_k^j(m)+c(\mathbf{z}_k)$. Here, $c(\mathbf{z}_k)$ is the clutter intensity. In part iii), the Bernoulli components for local hypothesis h^i of the track i is components as

$$f_{\mathrm{u},k}^{0,i,h^i}(\mathbf{x},m)=\frac{(1-p_{\mathrm{D},k}(\mathbf{x},m))f_{\mathrm{p},k}^{i,h^i}(\mathbf{x},m)}{\sum_{m'}e_k^{0,i,h^i}(m')}, \tag{10}$$

$$r_{\mathrm{u},k}^{0,i,h^i}=\frac{r_{\mathrm{p},k}^{i,h^i}\sum_m e_k^{0,i,h^i}(m)}{v_k^{0,i,h^i}(\emptyset)},\ w_k^{0,i,h^i}=w_{k-1}^{i,h^i}v_k^{0,i,h^i}(\emptyset), \tag{11}$$

where $e_k^{0,i,h^i}(m)=\int(1-p_{\mathrm{D},k}(\mathbf{x},m))f_{\mathrm{p},k}^{i,h^i}(\mathbf{x},m)\mathrm{d}\mathbf{x}$, and $v_k^{0,i,h^i}(\emptyset)=1-r_{\mathrm{p},k}^{i,h^i}+r_{\mathrm{p},k}^{i,h^i}\sum_m e_k^{0,i,h^i}(m)$. In part iv), each Bernoulli component of local hypothesis h^i of the track i associated with the measurement $\mathbf{z}_k^j\in\mathcal{Z}_k$ will have $r_{\mathrm{u},k}^{j,i,h^i}=1$, $w_{\mathrm{u},k}^{j,i,h^i}=w_{\mathrm{p},k}^{i,h^i}v_k^{j,i,h^i}(\{\mathbf{z}_k^j\})$, and

$$f_{\mathrm{u},k}^{j,i,h^i}(\mathbf{x},m)=\frac{p_{\mathrm{D},k}(\mathbf{x},m)f_{\mathrm{p},k}^{i,h^i}(\mathbf{x},m)g(\mathbf{z}_k^j|\mathbf{x},m)}{\sum_{m'}e_k^{j,i,h^i}(m')} \tag{12}$$

where $e_k^{j,i,h^i}(m')=\int p_{\mathrm{D},k}(\mathbf{x},m)f_{\mathrm{p},k}^{i,h^i}(\mathbf{x},m)g(\mathbf{z}_k^j|\mathbf{x},m)\mathrm{d}\mathbf{x}$. We also introduce $v_k^{j,i,h^i}(\{\mathbf{z}_k^j\})=r_{\mathrm{p},k}^{i,h^i}\sum_m e_k^{j,i,h^i}(m)$ for later use.

IV. Results

Setup: During $K=40$ time steps with a measurement interval of 500 ms, a vehicle UE is moving, with the initial position at $[70.7285,0,0]^{\mathrm{T}}$ m, driving in a circle around the BS (located at $[0,0,40]^{\mathrm{T}}$ m) with radius about 70.7285 m. We set the measurement noise covariance to $R=\mathrm{diag}\,(1{,}4\cdot10^{-4},4\cdot10^{-4},4\cdot10^{-4},4\cdot10^{-4})$. There are four VAs and four SPs in the environment. The survival probability is assumed to be constant $p_{\mathrm{S}}(m)=p_{\mathrm{S}}=0.99$ and the detection probability $p_{\mathrm{D}}=0.9$ within the FoV, where the SP FoV is $r_{\mathrm{FoV}}=50$ m the VAs are always visible. The clutter intensity is uniform with c(z)= $\lambda(\mathrm{R}_{\max}\pi^4)$, the clutter intensity $\lambda=1$, $\mathrm{R}_{\max}=200$ m. We set the birth weight $\eta_{\mathrm{B},k}(m)=2\cdot10^{-6}$ for $m=\{\mathrm{VA},\mathrm{SP}\}$. *Discussions:* Fig. 2 shows the average GOSPA of the VA and SP for the MM-PMBM compared to the MM-PHD [4]. In Fig. 2a, the average GOSPA of the VA is shown, and both VA GOSPAs for the MM-PMBM and MM-PHD go down over time. The number of detected VAs for the MM-PHD is larger than the true cardinality of VAs since the closely located SPs generate false alarm in the VA map. In the other hand, the MM-PMBM is robust to false alarm compared to the MM-PHD. In Fig. 2b, the average GOSPA of the SP is shown, and both SP GOSPAs also decrease over time. We confirm that the MM-PMBM can distinguish the two objects that are closely located, and thus the MM-PMBM significantly improve the SP mapping accuracy. Finally, it is confirmed that the MM-PMBM is also robust to missed detections as well as false alarm.

V. Conclusions

We present and evaluate the efficient framework of the MM-PMBM for 5G mapping, representing propagation of 5G mmWave signals. From the results, it is confirmed that the MM-PMBM address the challenges of the 5G mapping. We demonstrated that the MM-PMBM enhances the mapping performance compared to the MM-PHD.

Acknowledgement

This work was supported, in part, by the MSIT (Ministry of Science and ICT), Korea, under the ITRC (Information Technology Research Center) support program (IITP-2020-2017-0-01637) supervised by the IITP (Institute for Information & Communications Technology Planning & Evaluation), and by Institute of Information & Communications Technology Planning & Evaluation (IITP) grant funded by the Korea government (NFA) (No. 2019-0-01325, Developed of wireless communication tracking based location information system in disaster scene for fire-fighters and person who requested rescue).

References

[1] H. Kim, H. Wymeersch, N. Garcia, G. Seco-Granados, S. Kim, 5G mmWave vehicular tracking, in: Proc. IEEE 52nd Asilomar Conf. Signals, Syst., Comput., Pacific Grove, CA, USA, 2018, pp. 541–547.

[2] J. Mullane, B.-N. Vo, M. D. Adams, B.-T. Vo, A random-finite-set approach to Bayesian SLAM, IEEE Trans. Robot. 27 (2) (2011) 268–282.

[3] A. F. Garcıa-Fernandez, J. L. Williams, K. Granstrom, L. Svensson, Poisson multi-Bernoulli mixture filter: Direct derivation and implementation, IEEE Trans. Aerosp. Electron. Syst. 54 (4) (2018) 1883–1901.

[4] H. Kim, K. Granstrom, L. Gao, G. Battistelli, S. Kim, H. Wymeersch, 5G mmWave cooperative positioning and map- ping using multi-model PHD, IEEE Trans. Wireless Commun. 19 (6) (2020) 3782–3795.

[5] M. Beard, B. T. Vo, B.-N. Vo, S. Arulampalam, A partially uniform target birth model for Gaussian mixture PHD/CPHD filtering, IEEE Trans. Aero. Electron. Syst, 49 (4) (2013) 2835–2844.